JOURNAL OF ENVIRONMENTAL SCIENCES XX (2016) XXX–XXX

Available online at www.sciencedirect.com

ScienceDirect

www.elsevier.com/locate/jes

JES JOURNAL OF ENVIRONMENTAL SCIENCES

www.jesc.ac.cn

# MgO-based adsorbents for $CO_2$ adsorption: Influence of structural and textural properties on the $CO_2$ adsorption performance

*Gutiérrez-Bonilla Elvira*[1,2], *Granados-Correa Francisco*[1,*], *Sánchez-Mendieta Víctor*[2], *Morales-Luckie Raúl Alberto*[2]

1. *National Institute of Nuclear Research, Department of Chemistry, A.P. 18-1027, Col. Escandón, Miguel Hidalgo Delegation, Zip Code 1180 México D.F., México. E-mail: elvisboni02@hotmail.com*

2. *Autonomous University of México State, Faculty of Chemistry, Colón avenue, intersection with ride Tollocan s/n Toluca, México, México*

ARTICLE INFO

*Article history:*
Received 14 July 2016
Revised 20 September 2016
Accepted 12 November 2016
Available online xxxx

*Keywords:*
$CO_2$ adsorption
MgO-based adsorbents
Porous materials
Solution–combustion synthesis
Ball-milling process
Textural properties

ABSTRACT

A series of MgO-based adsorbents were prepared through solution–combustion synthesis and ball-milling process. The prepared MgO-based powders were characterized using X-ray diffraction, scanning electron microscopy, $N_2$ physisorption measurements, and employed as potential adsorbents for $CO_2$ adsorption. The influence of structural and textural properties of these adsorbents over the $CO_2$ adsorption behaviour was also investigated. The results showed that MgO-based products prepared by solution–combustion and ball-milling processes, were highly porous, fluffy, nanocrystalline structures in nature, which are unique physico-chemical properties that significantly contribute to enhance their $CO_2$ adsorption. It was found that the MgO synthesized by solution combustion process, using a molar ratio of urea to magnesium nitrate (2:1), and treated by ball-milling during 2.5 hr (MgO-BM2.5h), exhibited the maximum $CO_2$adsorption capacity of 1.611 mmol/g at 25°C and 1 atm, mainly via chemisorption. The $CO_2$ adsorption behaviour on the MgO-based adsorbents was correlated to their improved specific surface area, total pore volume, pore size distribution and crystallinity. The reusability of synthesized MgO-BM2.5h was confirmed by five consecutive $CO_2$ adsorption–desorption times, without any significant loss of performance, that supports the potential of MgO-based adsorbent. The results confirmed that the special features of MgO prepared by solution–combustion and treated by ball-milling during 2.5 hr are favorable to be used as effective MgO-based adsorbent in post-combustion $CO_2$ capture technologies.



## Introduction

It is well documented that carbon dioxide ($CO_2$) is the most significant greenhouse gas that mainly contributes to global warming. In the past five decades, atmospheric $CO_2$ emissions have been increased due to the accelerated industrial growth and technological development, resulting in a potential threat for the environment and ecosystems (Shafeeyan et al., 2015). The main anthropogenic sources of $CO_2$ emissions are attributed to the excessive fossil materials combustion such as carbon, oil and natural gas in the energy production and in many industrial processes (Bhagiyalakshmi et al., 2011). In

* *Corresponding author*. E-mail: francisco.granados@inin.gob.mx (Granados-Correa Francisco).

http://dx.doi.org/10.1016/j.jes.2016.11.016
1001-0742/

Please cite this article as: Elvira, G.-B., et al., MgO-based adsorbents for $CO_2$ adsorption: Influence of structural and textural properties on the $CO_2$ adsorption performance, J. Environ. Sci. (2016), http://dx.doi.org/10.1016/j.jes.2016.11.016

this context, inevitably due to the fact that fossil fuels will be the predominantly worldwide power supply, it is necessary to take urgent measures to reduce the high $CO_2$ concentrations in the atmosphere at great scale (Ello et al., 2013). As a consequence, currently, there are different $CO_2$ capture technologies for these purposes, including adsorption process, membrane separation, cryogenic methods, and so on. Among $CO_2$ capture technologies, the $CO_2$ adsorption using porous solid adsorbents has been receiving much attention because of their advantages, such as low regeneration energy requirements, no liquid waste, low cost, both pressure swing adsorption and temperature swing processes are widely used (Harrison, 2004). Indeed, also has attracted the researchers' attention due to that can to be designed and studied a great variety of potential $CO_2$ adsorbents of varied nature, cheap, and renewable for use in large-scale post combustion technologies. In this scenario, many solid porous materials have been widely recognized and used as potential adsorbents for $CO_2$ adsorption, including activated carbons (Houshmand et al., 2012), zeolites (Siriwardane et al., 2005), amine compounds (Saiwana et al., 2014), organometallic networks (Liu et al., 2012), metal oxides (Busca and Lorenzelli, 1982), and hydrotalcites (Radosław et al., 2015), among others.

Amid these above adsorbents listed, metal oxides are promising options for suitable $CO_2$ adsorbents and have a great potential in the future due to their easy accessibility and favorable thermodynamic properties (Kumar et al., 2015). However, the selection criteria of potential metal oxides for a large-scale application, entail their $CO_2$ capture capacity, adsorption rate, thermal stability, regeneration heat, availability, cost, textural and structural properties (Kumar and Saxena, 2014). Specifically, the alkaline-earth metal oxide (MgO) is widely used in many technological applications as: catalysis, toxic waste remediation, additive in refractory, optically transparent ceramic windows, adsorbent for many pollutants, paint and superconductor products, among others (Jin et al., 2012). MgO is a white hygroscopic solid mineral that occurs naturally as periclase, is a source of magnesium, is a non-toxic and environmentally friendly material with higher surface reactivity and adsorption capacity, and is a suitable adsorbent for anions and cations from aqueous solution due to its favorable electrostatic attractive mechanism (Crittenden et al., 2005). In recent studies, MgO has been widely explored for $CO_2$ capture, and has been recognized as one of the most promising adsorbents for $CO_2$ adsorption together with CaO, because these metallic oxides combine with $CO_2$ present in the flue gas post-combustion and form thermodynamically stable carbonates in a reversible reaction; heating the carbonates regenerates the respective oxides and thus liberates almost pure stream of $CO_2$ that it can be directly transported to a storage site, and subsequently be used technologically (Kumar and Saxena, 2014). It has been reported that MgO can adsorb $CO_2$ below 200°C by carbonation, and can be regenerated by calcination at relatively low temperature compared with conventionally-used CaO subjected to cyclic $CO_2$ capture from flue gases, which makes it very desirable because it is widely accepted that there is a large scope for cost reduction and energy efficiency improvements in $CO_2$ capture systems (Wang et al., 2011). In general, many metal oxides can qualify for $CO_2$ capture application, however, one of the key factors in gas–solid reaction is their textural, morphological and structural properties that are essential forenhancing their $CO_2$ adsorption. Thus, synthesis of MgO with improved specific surface area, nanocrystalline size, large total pore volume and narrow size pore distribution is of great interest as $CO_2$ adsorptive materials. The direct relation of these MgO physico-chemical properties with the $CO_2$ capture behavioris still not completely resolved and needs to be investigated.

On the other hand, extensive synthesis methods have been followed to obtain MgO products with porous structures and multiple morphologies, including the precipitation method (Janet et al., 2007), hydrothermal synthesis (Zhao et al., 2011), and sol–gel method (Kim et al., 2005). It is well known that the employed synthesis method and the chemical precursors to prepare powders, have a large influence on the textural and structural characteristics of materials such as porosity, specific surface area, particle size, crystallinity, between others. Particular desirable properties of compounds in their use as adsorbents are mainly extensive specific surface area that means many active sites for contaminant adsorption and a higher porous nature, which plays an important role on $CO_2$ capture. Therefore, it is evident from the above that there is a need for a continuous improvement and development of new and potential adsorbents for gaseous, aqueous, and non-aqueous streams. Currently, the novel solution–combustion synthesis is widely used for preparing different oxide powders with high purity, high yield, large specific surface areas, and good quality mesoporous structures at short times compared to other conventional synthesis methods. Furthermore, this method is safe, simple and instantaneous for the facile fabrication of nanopowders, indeed, the solution–combustion synthesis requires simple equipment with energy saving (Toniolo et al., 2010). For this method are required high temperatures for the exothermic redox reactions and achieve the decomposition of the metal salt and the organic fuel for products formation. Therefore, extensive studies have been conducted to investigate solution–combustion synthesis of many metallic oxide powders using urea as the most commonly used chemical fuel, and some other fuels such as: starch, glycine and sorbitol (Bhatta et al., 2015; Bai et al., 2011; Devaraja et al., 2014; Granados-Correa and Bonifacio-Martínez, 2014; Mantilaka et al., 2014).

On the other hand, recent advances in nanotechnology have made much interest in preparing metallic oxide nanocompounds. The mechanical ball-milling is an extensive method to obtain nanostructured materials; this mechanical ball-milling treatment allows to activate dry solids and, especially increase its specific surface area as well as improve properties (Janusz et al., 2010). Nanopowders show substantially enhanced adsorption characteristics superior to those of the conventionally prepared powders (Liang et al., 2001). It is important to note that the gas adsorption efficiency can increase with a decrease in the MgO powder size and crystallites. In fact, the high gas adsorption efficiency of nanoparticles is also caused by their large specific surface area, and structural defects on their surface. Furthermore, it has been shown that metallic oxides doped with doping-metals such as Fe, Ni, Cd, Ce, Co among others, show significant changes in their properties with respect to original materials. In

Please cite this article as: Elvira, G.-B., et al., MgO-based adsorbents for $CO_2$ adsorption: Influence of structural and textural properties on the $CO_2$ adsorption performance, J. Environ. Sci. (2016), http://dx.doi.org/10.1016/j.jes.2016.11.016

terms of the basis of these approaches, doped metallic oxides are of research interest because of its diverse properties, which originate from its structural characteristics. In this context, MgO doped adsorbents with significant doping-metals such as Fe and Ni are here systematically studied as new and potential solid adsorbents with improved properties that can be used to separate $CO_2$ effectively from flue gases generated by fossil fuel combustion. Their novel properties and/or improved performance can provide an additional contribution and effort to develop an efficient $CO_2$ capture method.

The aim of this work was to prepare a series of MgO-based adsorbents by solution–combustion and ball-milling processes, the introduction of Fe and Ni dopants into the MgO crystal structure has also been considered as efficient approach to improve its $CO_2$ capture. Then, the obtained MgO materials were used comparatively as potential adsorbents for $CO_2$ adsorption. In this context, their $CO_2$ adsorption behaviors were interpreted in light of a detailed textural, morphological, and structural characterization. Indeed, the $CO_2$ desorption and regeneration ability of the best resulted $CO_2$ adsorbent was also studied.

## 1. Experimental

### 1.1. Materials

Magnesium nitrate hexahydrate ($Mg(NO_3)_2{\cdot}6H_2O$, 99.0% purity) and urea ($CH_4N_2O$, 99.4% purity) were purchased from Mallinckrodt ACS, and Fermont ACS, Phillipsburg, NJ, respectively, and used as such without any purification, distilled water was used throughout the synthesis of MgO nanocompounds. To obtain the MgO–Fe and MgO–Ni nanocomposites, iron (Fe, 99.5% purity) and nickel (Ni, 99.5% purity) elements of analytical grade were used and obtained from Sigma-Aldrich, St. Louis, MO. All used gases in this study were supplied by Infra México, México, with the following specifications: carbon dioxide extra dry ($CO_2$, 99.9% purity), nitrogen ($N_2$, 99.9% purity), and helium (He, 99.9% purity).

### 1.2. Synthesis of MgO-based adsorbents

MgO-based adsorbents were synthesized *via* solution–combustion method and treated by ball-milling process. In order to establish the best experimental conditions for MgO formation with large specific surface area and porosity, by solution–combustion synthesis, different molar ratios of chemical precursor's urea as chemical fuel and magnesium nitrate as oxidizer (1:1 to 2.5:1) at 800°C during 5 min were proven. For this purpose, determined quantities of urea and magnesium nitrate were placed into 50 mL porcelain crucible and dissolved with 1 mL of distilled water. The obtained homogeneous mixture was heated at 260°C during 20 min with help of electric grill for water evaporation, obtaining a consistent material with gel appearance. Then, the resulting gel was calcined for 5 min into muffle furnace at 800°C. The water effect in the MgO combustion synthesis also was studied, for this purpose, to resulting material different amounts of distilled water (0.5 to 2.5 mL) were added, prior to calcination at 800°C for 5 min. On the other hand, the MgO sample obtained by solution–combustion was ball-milling by using a stainless ball mill Spex type with a ratio mass-steel balls of 6:1 into container at different time periods (2.5 to 10.0 hr). Indeed, the MgO–Fe and MgO–Ni nanocomposites were prepared also by ball-milling at different milling time periods from 2.5 to 10.0 hr by using a ratio percent weigh MgO to metal element of 98:2 wt.%. Finally, the prepared MgO-based adsorbents were stored in glass vials, sealed and labeled for further characterization and $CO_2$ adsorption experiments. The resulting samples were labeled according to the preparation processes as: MgO synthesized by solution–combustion process (MgO-SC), MgO synthesized by solution–combustion and treated by ball-milling (MgO-BM), MgO synthesized by solution–combustion and mixed with elemental Fe by ball-milling (MgO-Fe), and MgO synthesized by solution–combustion and mixed with elemental Ni by ball-milling (MgO–Ni) respectively. In the present study, in order to investigate the textural and structural material effects on the $CO_2$ adsorption behavior, the most significant textural properties of obtained materials such as: large specific surface area, narrow pore size distribution and large total pore volume, were selected and subsequently used to study their $CO_2$ adsorption behavior at different pre-established temperatures and pressures.

### 1.3. MgO-based adsorbents characterization

Phase composition and crystalline structures of selected prepared MgO-based adsorbents were identified by X-ray diffraction (XRD) using a SIEMENS D-5000 diffractometer, Madison, WI, with Cu-Kα radiation ($\lambda$ = 1.54060 Å). The crystalline MgO structures were identified according to the Joint Committee of the Powder Diffraction Standard (JCPDS) cards. The average crystallite sizes of these MgO-based compounds were determined by means of the Sherrer's equation, applied to the major XRD peaks (Granados-Correa et al., 2016). The morphologies and the elemental chemical composition of the MgO samples were studied by scanning electron microscopy (SEM, JEOL, Tokyo, Japan) using a JEOL-JSM-5900LV instrument equipped with an energy dispersive X-ray analysis (EDX) detector using OXFORD microprobe. Brunauer–Emmett–Teller (BET) specific surface areas ($S_{BET}$), mean pore diameters ($d_p$), and total pore volumes ($V_{Tp}$) of the prepared MgO nanomaterials were calculated by $N_2$ physisorption measurements. Nitrogen adsorption–desorption isotherms were measured at 77 K, and the pore size distributions were determined using the Barrett–Joyner–Halenda (BJH) method. All $N_2$ physisorption measurements were made on a Micromeritics BELSORP MAX Inc. Osaka, Japan volumetric adsorption analyzer. Prior of $N_2$ measurements, samples were degasified in a nitrogen stream at 473 K for 3 hr.

### 1.4. $CO_2$ adsorption experiments

$CO_2$ adsorption experiments were carried out on MgO-based adsorbents by using a stainless reactor Parr 4592 of 50 mL capacity coupled with a temperature-controlled system. Approximately 15 mg of each material was used during each experiment. For this purpose, the samples were loaded into the reactor and degassed under vacuum at 325°C by 30 min. The equilibrium experiments were carried out at temperatures of

Please cite this article as: Elvira, G.-B., et al., MgO-based adsorbents for $CO_2$ adsorption: Influence of structural and textural properties on the $CO_2$ adsorption performance, J. Environ. Sci. (2016), http://dx.doi.org/10.1016/j.jes.2016.11.016

25, 40, 60 and 80°C and at pressures of 1, 5, 10 and 15 atm for 30 min. The amount of millimoles of $CO_2$ adsorbed per gram of adsorbent (mmol/g), was obtained on the basis of the weight loss of $CO_2$ that is adsorbed in the nanocompounds by using a TA Instruments SDT Q600 thermo gravimetric analyzer (New Castle, DE) coupled to mass spectrum analyzer TA Instruments model LLC (New Castle, DE), heating the samples at a rate of 20°C/min up to 850°C in helium atmosphere at a flow rate of 100 mL/min.

## 2. Results and discussion

### 2.1. Synthesis

It was found the optimum conditions of MgO synthesis *via* solution–combustion process, by using a molar ratio (2:1) of chemical precursor's urea to magnesium nitrate, and using 1.5 mL of distilled water prior to calcination at 800°C during 5 min. In this solution–combustion synthesis, a rapid chemical process based on the explosive decomposition of urea as fuel was carried out. This decomposition provides heat for calcination and produces high temperatures since fuel-to-oxidant ratio in an oxidant-fuel mixture has a significant effect on combustion synthesis (Granados-Correa et al., 2008). Moreover, theoretically, a stoichiometric redox mixture could produce maximum energy during combustion. Then, in this work, MgO was fabricated for better textural properties by using various redox mixtures as described in the Experimental section. As a consequence, a molar ratio of urea to magnesium nitrate (2:1) was established as the best MgO solution–combustion reaction. In order to find the yield for this reaction to obtain MgO, yielding product was determined as a function of the fuel-to-oxidant ratio according to Jain and Adiga (1981). The balanced equation for the combustion reaction in this study can be written as Eq. (1):

$$3\left[Mg(NO_3)_2\cdot 6H_2O\right]_{(s)} + 5CH_4N_2O_{(s)} \rightarrow 3MgO_{(S)} + 8N_{2(g)} + 5CO_{2(g)} + 28H_2O_{(g)} \quad (1)$$

In solution–combustion reaction for MgO powder formation (Eq. (1)), there is a release of $N_2$, $CO_2$ and $H_2O$ molecules in excess, generating porous MgO with homogeneous fine particles of spherical shape. This was clearly confirmed by SEM observations. It is worthwhile to mention that in this reaction, urea acts as a chemical fuel, and $H_2O$ has a significant role for this porous structure formation of MgO powder, due to the exothermic reaction that is generated. According to previous investigations (Cai et al., 2009a, 2009b), urea was also used as precipitating agent. In agreement to Choong-Hwan and Ji-Yeon (2010) the principles of propellants and explosives for a redox reaction between a fuel and an oxidizer, the cation (carbon, hydrogen and oxygen) acts as fuel, and the metal nitrate anion (oxygen) acts as the oxidizer. Then, in this work, to know if the mixture is rich or poor in fuel, the oxidant-fuel mixture that is usually expressed in terms of elements stoichiometric coefficient ($\Phi_e$), was calculated using Eqs. (2) and (3) (Jain and Adiga, 1981).

$$\Phi_e = \frac{\sum(C_{oxi})\times(v)}{(-1)\sum(C_{red})\times(v)} \quad (2)$$

$$\Phi_e = \frac{\left[(6\times 10^{-3}\times 2Mg) + (2\times 0N) + (0.0404\times 2O) + (0.0333\times 2O)\right]}{(-1)\left[(0.0333\times -4C) + (0.1332\times -1H) + (2\times 0N)\right]} \quad (3)$$

where, $C_{oxi}$ is the coefficient of oxidizing elements in specific formula; $C_{red}$ is the coefficient of oxidizing elements in specific formula; $v$ is the valency. $\Phi_e = 1$ corresponds to the stoichiometric ratio, $\Phi_e > 1$ indicates a poor mixture in fuel and $\Phi_e < 1$ is a rich fuel mixture. The results indicated that to obtain a stoichiometric mixing of the oxidizing-reducing species ($\Phi_e = 1$), the molar ratio of fuel-oxidizer must be 5:3 as shown in Eq. (1). However, the combustion reaction of this work was fuel rich with a molar ratio urea to magnesium nitrate (2:1) with ($\Phi_e = 0.598$), this fuel rich can benefit the MgO formation due to the fact that more energy exists during the combustion of powders, which allowed to obtain a high yield, 99.42%, from the reaction. Therefore, this optimum performance made the process feasible by solution–combustion synthesis to successfully obtain MgO powders with increased porosity and specific surface area. The as-prepared MgO nanopowders by solution–combustion in this study were compared with another reported MgO powders from urea as fuel, and these results are in agreement with Maliyekkal et al. (2010) and Rao and Sunandana (2008), highlighting in these cases that all MgO samples prepared by this fast method, present a higher porous nature, small crystalline size, and high purity.

### 2.2. Characterization

Fig. 1 shows the X-ray diffraction patterns for all MgO-based adsorbents studied here. These materials only show the characteristic peaks assigned to crystalline MgO, with periclase cubic structure according to the JCPDS 01-087-0651 file. It has been reported that the ball-milling process has an important impact on the crystallinity of materials, attributed to the high pressure and high temperatures generated locally during the milling process in the ceramic powders (Granados-Correa et al., 2016). Then, an important change in crystallinity of MgO-SC sample after ball-milling process was observed. In Fig. 1c and d, Fe and Ni element phases cannot be recognized by XRD patterns

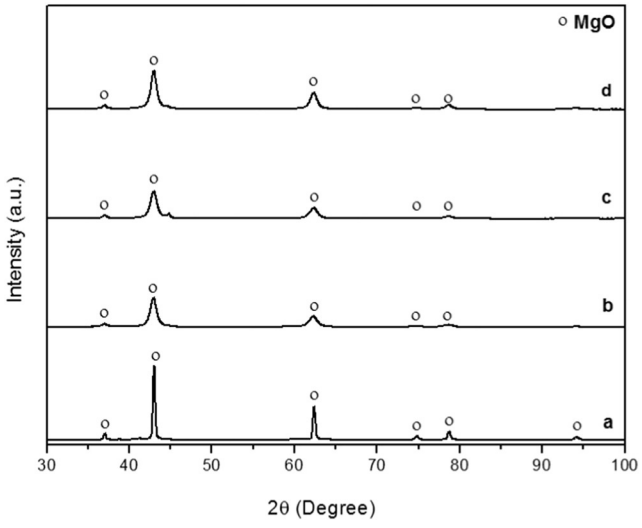


**Fig. 1 – X-ray powder diffraction patterns of MgO-based adsorbents samples: (a) MgO-SC, (b) MgO-BM2.5h, (c) MgO–Fe, and (d) MgO–Ni.**

Please cite this article as: Elvira, G.-B., et al., MgO-based adsorbents for $CO_2$ adsorption: Influence of structural and textural properties on the $CO_2$ adsorption performance, J. Environ. Sci. (2016), http://dx.doi.org/10.1016/j.jes.2016.11.016

due to their lower weight ratios (98 wt.% MgO sample: 2 wt.% Fe or Ni respectively).The average crystallite sizes of all studied MgO-based adsorbents were found to be 40.73 nm for MgO-SC sample, 8.61 nm for MgO-BM2.5h, and 10.13 and 10.49 nm for MgO–Fe and MgO–Ni samples, respectively. The discrepancy of MgO-based adsorbent crystallinity is a result of the intense shocks of milling media (steel balls) on MgO particles or due to some disaggregation of MgO-SC particles (Singh et al., 2009).

It was observed that the specific surface area for MgO-BM2.5h sample with lower average crystallite size (8.61 nm) was increased, because the solid milling favors particle fragmentation. Therefore, results revealed that there is a clear change in structure and specific surface area when the MgO-SC sample is ball-milled, which can be expected that would increase its $CO_2$ capture. The microstructural effect of ball-milling time over MgO ball milling sample, also was studied during 5, 7.5 and 10 hr respectively, and the results indicated that for a longer ball-milling time, a decrepitation occurred, which not caused a decrease of crystallite size, but generated ultrafine powders. Therefore, a short milling time of 2.5 hr is the most suitable route for producing MgO nanocrystalline adsorbent with improved structural and textural characteristics for efficient $CO_2$ adsorption. According to Valverde et al. (2014), a reduction of metallic oxide (CaO) crystallinity by ball-milling favors diffusion and serves to promote recarbonation in accordance with the $CO_2$ capture subject to carbonation/calcination cycles at Ca-looping, where a mechanism for $CaCO_3$nucleation on the CaO surface in islands has been proposed (Kumar et al., 2015). In this study, the MgO behavior is associated to that of CaO behavior. Therefore, it is widely accepted that a gas–solid carbonation reaction occurs for the MgO-$CO_2$ reaction. According to Kumar and Saxena (2014), MgO particles are surrounded by $CO_2$ molecules and react to form $MgCO_3$. However, $MgCO_3$ forms an impervious layer around unreacted MgO particles and hampers the further diffusion of $CO_2$ molecules, as can be seen in Fig. 2, for a schematic$CO_2$ adsorption mechanism on mesoporous MgO adsorbent.

It is recognized that when $CO_2$ molecules make contact with the metallic oxide surface as a $CO_2$ adsorbent, they will be in contact with two surface types: the metal oxide surface and the metal carbonate surface; when $CO_2$ molecules make contact with the metal oxide surface, carbonation directly occurs, which is thermodynamically stable at temperature and pressure ambient conditions, while for a metal carbonate surface happens by diffusion through this layer of carbonates. It is showed that the carbonation in this stage is mainly driven by solid state diffusion, which is of practical interest. Therefore, this MgO crystal structure role is necessary in order to lead the complete carbonate conversion of MgO. Thus, a correlation between the crystallinity changes of MgO-based adsorbents with their $CO_2$ adsorption capacities is expected because the ball-milling process causes a not very orderly atom structure in the particles, which can enhance the $CO_2$ adsorption capacity.

Fig. 3 shows the MgO-based adsorbent morphology. The MgO-SC sample (Fig. 3a) is characterized by spherical shape particles of soft surface texture with sizes ranging from 0.5 to 5 μm. EDX analysis results indicated that MgO-SC powders are composed of Mg (62.42 at.%) and O (37.57 at.%), showing

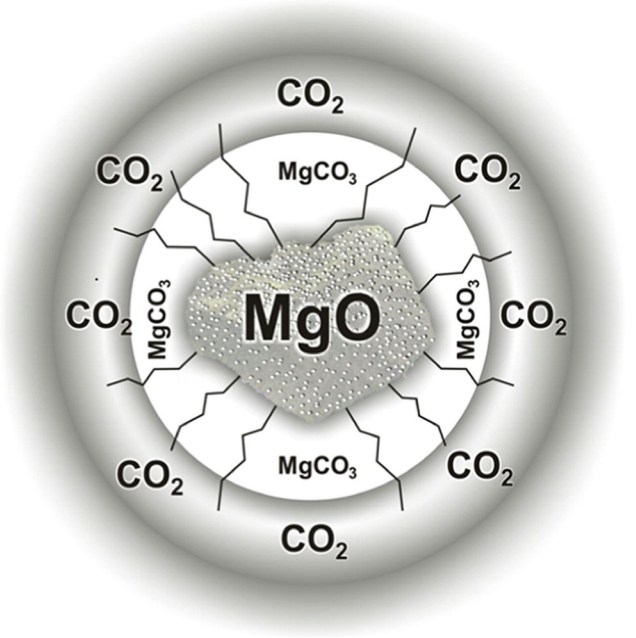


**Fig. 2 – Schematic $CO_2$ chemisorption mechanism on mesoporous MgO-based adsorbent.**

that the desired material was obtained by using solution–combustion synthesis only. The MgO-BM2.5h sample (Fig. 3b), exhibited spongy and porous aggregates of irregular shapes with rough surfaces due to the fragmentation of the dust trapped during collision of balls against the container walls during ball-milling process. In Fig. 3c and d the morphological changes of MgO–Fe and MgO–Ni samples were exhibited; in these micrographs the particles are characterized by irregular shapes with slightly rounded edges and rough textures, also clearer fine particles were observed. EDX analysis showed a heterogeneous distribution of Fe (2.12 at.%) and Ni (0.92 at.%) in MgO samples, indicating that Fe and Ni elements are built in the crystal structure of MgO-Fe and MgO-Ni samples, respectively, with well-particle dispersion which can produce reactive powders. Indeed, the sizes of particle are considered in the nanometric range. Henceforth, a narrow particle size distribution generates more specific surface area, meaning more active sites for $CO_2$ adsorption. In order to achieve high efficiency of $CO_2$ capture in advanced technologies based in the $CO_2$ capture by carbonation/calcination of metallic oxides for $CO_2$ looping cycles, the systems can adopt a process configuration that consists of using two interconnected circulating fluidized bed reactors as a carbonator and as a calciner, which allows working with higher surface speeds of gas and higher circulations of the solid adsorbent (Abanades et al., 2005). For these purposes, surface properties of MgO-based adsorbents such as specific surface area, particle size, and porosity are very critical parameters that favor the carbonation process of metallic oxides, increasing the $CO_2$ adsorption efficiency.

The $N_2$-physisorption measurement results of prepared MgO-based adsorbents are listed in Table 1. It was observed that the MgO-BM2.5h sample considerably increased their BET specific surface area, and total pore volume in comparison

Please cite this article as: Elvira, G.-B., et al., MgO-based adsorbents for $CO_2$ adsorption: Influence of structural and textural properties on the $CO_2$ adsorption performance, J. Environ. Sci. (2016), http://dx.doi.org/10.1016/j.jes.2016.11.016

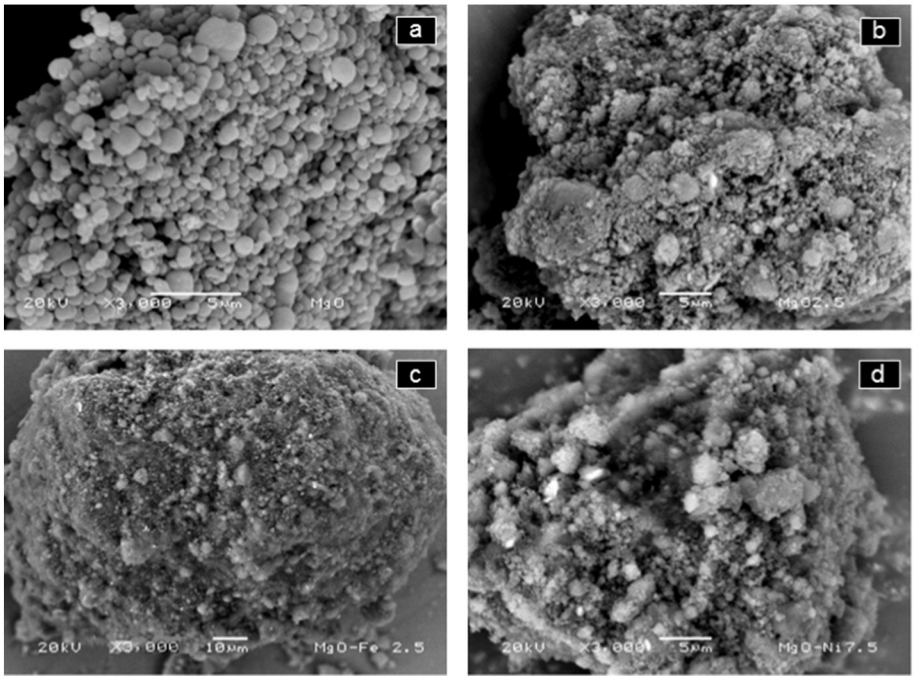


**Fig. 3 – SEM micrographs of MgO-based adsorbents: (a) MgO-SC, (b) MgO-BM2.5h, (c) MgO–Fe, and (d) MgO–Ni.**

with MgO-SC sample from 5.71 $m^2/g$ and 0.0289 $cm^3/g$ to 15.24 $m^2/g$ and 0.1347 $cm^3/g$ respectively, and the pore size diameter was increased from 12.12to 21.52 nm. The obtained results revealed an aggregation of particles generated by the ball-milling process, which led to the moderate pore formation. In accordance with Bhatta et al. (2015), MgO mesoporous with large BET specific surface areas and mesopore size distribution is considered a good adsorbent of $CO_2$ because it exhibits better selectivity.

The adsorbent pore size distribution has a significant influence on $CO_2$ adsorption since it can affect the transport of mass, the available pore space of $CO_2$ adsorbents would increase to some extent, leading to a faster diffusion of $CO_2$ in the pores. Fig. 4 shows the pore size distributions of MgO based adsorbents. The MgO-SC and MgO-BM2.5h samples have large pore size distributions with average pore diameters of 9.20 and 21.52 nm, respectively (Fig. 4a and b); however, the MgO–Fe and MgO–Ni samples revealed pore size distributions relatively narrow, with average pore diameters of 9.20 and 4.20 nm, respectively (Fig. 4c and d). It was observed in our results that all MgO-based adsorbents exhibited mesoporous structures for high selectivity towards $CO_2$ molecules of 0.33 nm of kinetic radius, enough for $CO_2$ molecule diffusion inside the porous of MgO-based adsorbents; in this way, intraparticle diffusion improves the $CO_2$ capture process, because it facilitates the access of $CO_2$ molecules to pore active sites in pore walls. It is known that for chemisorption, $CO_2$ molecule has to diffuse into the adsorbent and interacts with the internal adsorbent surface. In this context, an excellent chemical adsorbent should not only have high specific surface area for chemisorption but also have appropriate pore size distribution for facilitating the $CO_2$ diffusion in the adsorbent pore structure (Song et al., 2016). In our case, the MgO-BM2.5 sample with a wide pore size distribution of 21.52 nm exhibited the best $CO_2$ adsorption performance than the other studied MgO-based adsorbents. In fact, the

**Table 1 – Textural properties of MgO-based adsorbents synthesized by solution combustion and ball-milling processes.**

| Sample | $S_{BET}$ ($m^2/g$) | $V_{Tp}$ ($cm^3/g$) | $d_p$ [a] (nm) |
|---|---|---|---|
| MgO-SC | 5.71 | 0.0289 | 12.12 |
| MgO-BM2.5h | 15.24 | 0.1347 | 21.52 |
| MgO–Fe | 15.85 | 0.1387 | 9.20 |
| MgO–Ni | 30.83 | 0.1588 | 4.20 |

$S_{BET}$: superficial area; $V_{Tp}$: total pore volume; $d_p$: average pore diameter.
[a] Barrett–Joyner–Halenda (BJH) method.

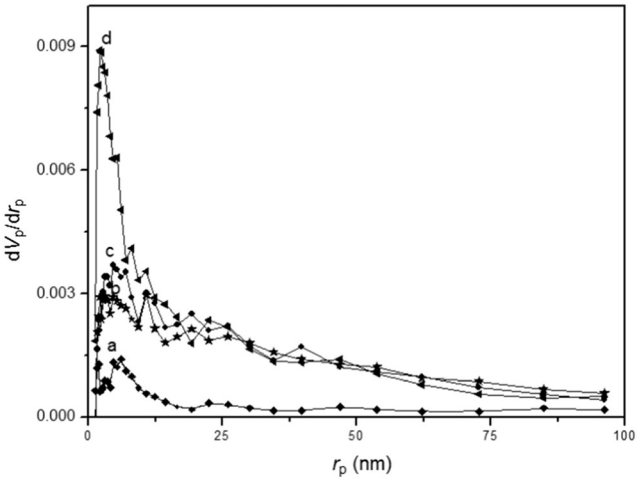


**Fig. 4 – BJH pore size distribution of MgO-based adsorbents: (a) MgO-SC, (b) MgO-BM2.5h, (c) MgO–Fe, and (d) MgO–Ni.**

Please cite this article as: Elvira, G.-B., et al., MgO-based adsorbents for $CO_2$ adsorption: Influence of structural and textural properties on the $CO_2$ adsorption performance, J. Environ. Sci. (2016), http://dx.doi.org/10.1016/j.jes.2016.11.016

mesoporous MgO is highly basic with well-ordered porous structure to expect high $CO_2$ adsorption.

Fig. 5 shows the $N_2$ adsorption–desorption isotherms for the as-prepared MgO nanocompounds. All these MgO-base adsorbents showed type IV isotherms according to the International Union of Pure and Applied Chemistry (IUPAC) classification (Abd-El-Hafiz et al., 2015), in accordance with this IUPAC isotherm classification, type IV isotherms are characteristics of mesoporous materials (2 nm < pore size < 50 nm). On the other hand, MgO-SC sample (Fig. 5a) shows a type H4 hysteresis. MgO-BM (Fig. 5b), MgO-Fe (Fig. 5c) and MgO-Ni (Fig. 5d) samples showed type H3 hysteresis in 0.4–1.0 $p/p_o$ range. Materials with type H3 and H4 hysteresis are usually solids that formed particle agglomerates and have existence of flexible pores with morphology of slit or plate type. Furthermore, the hysteresis formation begins in the middle part of the isotherms, indicative of a distribution of pore size which extends mainly to the mesopore size at $0.4 < p/p_o < 1$ (Adelkhani et al., 2011). Based on these findings, the presence of mesoporous structure in the prepared MgO-based adsorbents is confirmed, as was corroborated with the BJH results.

### 2.3. $CO_2$ adsorption

The $CO_2$ adsorption results on MgO-based adsorbents at 25°C, 1 atm, and 30 min of saturation time show that for MgO-SC, MgO-BM2.5h, MgO–Fe and MgO–Ni samples, maximum adsorption capacities of 0.39, 1.61, 0.90 and 1.50 mmol of $CO_2$ per gram of adsorbent were obtained, respectively. Fig. 6 show the thermal gravimetric analysis (TGA) curve and mass spectroscopy (MS) of $CO_2$ adsorption on studied MgO-based adsorbents. A weight loss of 7.09% for MgO-BM2.5h sample was observed (Fig. 6b), which was higher compared than MgO-SC (1.73 wt.%), MgO–Fe (3.99 wt.%) and MgO–Ni (6.64 wt.%) samples, respectively, due to their remarkably different textural and structural characteristics that were directly correlated with their $CO_2$ adsorption capacities. With respect to Mg–Ni and MgO–Fe performance difference, Table 1 showed that for MgO doped with Ni and Fe metals (MgO–Ni and MgO–Fe) samples, significant improvement of specific surface area, as well as the total pore volume was observed. In catalysis

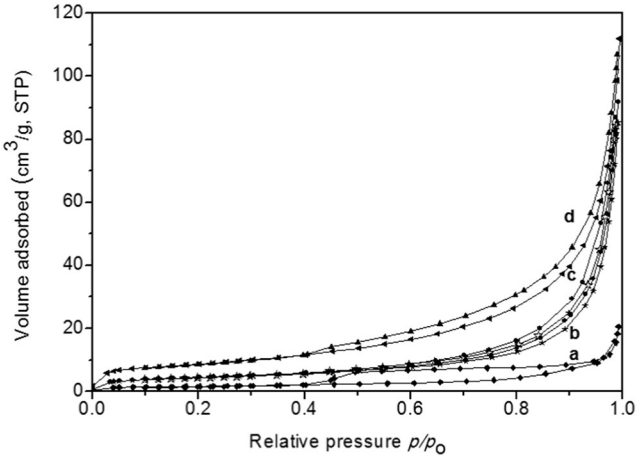


**Fig. 5 – Adsorption–desorption isotherms of MgO-based adsorbents: (a) MgO-SC, (b) MgO-BM2.5h, (c) MgO–Fe, and (d) MgO–Ni.**

field, doped metal oxides are widely investigated materials and novel doping-metals such as Fe and Ni have been proposed to improve the performance of metal oxide based adsorbents. In this case, catalytic activity and selectivity behaviors are linked to dopant acidity and basicity properties (Pighini et al., 2011). In fact, it has been demonstrated that nanocomposites can exhibit the multicomponent system properties in the same material (Singh et al., 2013). It has been shown that the Ni catalyst surface acidic or basic properties can significantly affect their $CO_2$ adsorption performance, favoring the $CO_2$ adsorption capacity on the MgO basic sites or inhibiting the $CO_2$ adsorption by the deposition of a solid carbonaceous residue when surfaces are in contact (Jeong et al., 2016). Moreover, to our knowledge, iron incorporated in metal oxides has an excellent redox ability to capture $CO_2$ under high temperatures; however, no study has been reported as $CO_2$ capture material at low and ambient temperatures. In our case, at ambient temperature, Fe powders can have the inconvenience of carbon deposition in the metallic oxide active sites during the $CO_2$ adsorption, causing the deactivation and textural destruction of MgO nanocompounds mixed with metallic powders as Fe, consequently resulting in a decrease in active sites due to the saturation with carbon species as was observed in MgO–Fe sample (Khajenoori et al., 2015; Ross, 2005; Wang et al., 2012). Thus, it was observed that after the introduction of Ni and Fe into MgO adsorbent, both of the specific surface areas and total pore volumes increase (Table 1), benefiting their $CO_2$ performance by increasing these important textural characteristics irrespective of their synthesis method. Additionally, the solid milling favored particle fragmentation which provides a large number of active sites, as well adding the corresponding Ni and Fe active sites. However, the corresponding average pore sizes decrease due to prolonged pore compaction caused by the ball-milling process, taking into account that MgO–Fe sample was ball-milling during 5.0 hr and MgO-Ni sample during 7.5 hr. Therefore, a significant influence of the doping element on the $CO_2$ adsorption behavior was revealed. Moreover, even if these samples are issued from the same precursor, doped samples allowed to increase or decrease the $CO_2$ adsorption capacity. Hence, the MgO-BM2.5h exhibited better $CO_2$ adsorption capacity due to their morphology, textural and microstructure properties. Moreover, this MgO-BM2.5h sample showed more abundant mesoporous structure to ensure that $CO_2$ molecules easily come into contact with the active sites that provide their extended specific surface area, improving the interaction between $CO_2$ gas molecules with the MgO-BM2.5h mesopores. According to Li et al. (2010), the enhanced interaction at mesopores gives rise to strong adsorption of $CO_2$, which finally improved the $CO_2$ adsorption capacity. Similarly, Bhagiyalakshmi et al. (2010), reported that MgO powders are highly basic and can adsorb $CO_2$ molecules in the active sites of MgO surface which are trapped into the pores by chemical reaction of MgO and $CO_2$ to form $MgCO_3$. Therefore, the specific surface area, total volume pore, average pore diameter, morphology and crystallinity were critically important in encouraging the $CO_2$ adsorption capacity on these MgO-based adsorbents studied here. MgO-BM2.5h powders are highlighted to be beneficial for potential applications in $CO_2$ adsorption under practical conditions at 25°C, 1 atm, and 30 min of saturation time.

Thermal decomposition process for the MgO-BM2.5h sample after $CO_2$ exposure was examined using TGA and differential scanning calorimetry (DSC) techniques. The TGA/DSC curves

Please cite this article as: Elvira, G.-B., et al., MgO-based adsorbents for $CO_2$ adsorption: Influence of structural and textural properties on the $CO_2$ adsorption performance, J. Environ. Sci. (2016), http://dx.doi.org/10.1016/j.jes.2016.11.016

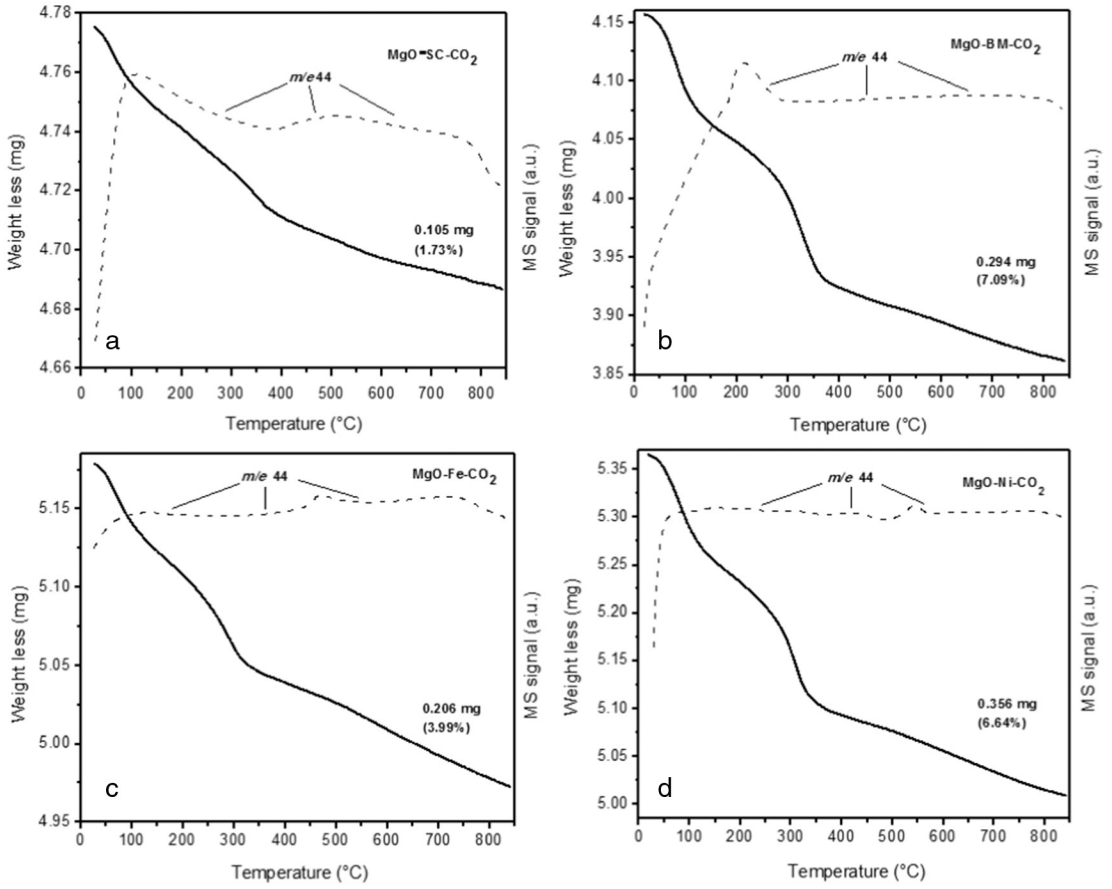


**Fig. 6 – TGA curves and MS $CO_2$ adsorption on MgO-based adsorbents: (a) MgO-SC, (b) MgO-BM2.5h, (c) MgO-Fe, and (d) MgO-Ni at 25°C and 1 atm. TGA: thermal gravimetric analysis; MS: mass spectroscopy.**

for $CO_2$desorbedon MgO-BM2.5h powders are shown in Fig. 7. It can be observed that in the DSC curve there is an endothermic peak at 99.5°C caused by the elimination of physically adsorbed water (Vu et al., 2014). At higher temperature, a second and third exothermic broad peaks from 150 to 750°C were observed, which are associated with carbonaceous material ($CO_2$) release. The small peak at around 370°C corresponds to weakly adsorbed $CO_2$ while the broad peak at around 330°C represents desorption of the strongly chemisorbed $CO_2$ (Bhagiyalakshmi et al., 2011). Subsequently, an endothermic peak is observed at around 800°C due to the complete MgO phase formation. From the TGA/DSC results, the release of $CO_2$ is due to $MgCO_3$ formation. This $CO_2$ adsorption on MgO-MM2.5h by carbonation was confirmed by FT-IR (FT: fourier transform; IR: infrared) analysis. Therefore, the TGA/DSC result indicates that $CO_2$ was chemisorbed on MgO-BM2.5h sample, and that at around 800°C a complete sharp regeneration of $CO_2$ was observed. Then, the obtained TGA/DSC results are suggested that chemisorption was mainly the mechanism that governs the $CO_2$ adsorption on MgO-BM2.5 adsorbent.

In order to analyze the carbonate formation, FT-IR analysis was performed. In Fig. 8, IR spectra are shown for a MgO-BM2.5h sample without further treatment (Fig. 8a), for MgO-BM2.5h sample degassed at 325°C during 30 min (Fig. 8b), and for MgO-BM2.5h sample after $CO_2$ adsorption. The FT-IR analysis of MgO-BM2.5h samples exhibits a typical metal oxide spectrum with significant difference between the fresh material, degasified material, and sutured material by $CO_2$. All spectra in Fig. 8a–c show four main adsorption bands: at 522 $cm^{-1}$, a remarkable adsorption band ranging from 1200 to 1700 $cm^{-1}$, a band at 2314 $cm^{-1}$, and at 3433 $cm^{-1}$ respectively. The bands at 522 and 3433 $cm^{-1}$ are assigned to the Mg–O bond and stretching vibrations of the O–H bond respectively (Devaraja et al., 2014). The IR adsorption bands of hydroxyl groups (water

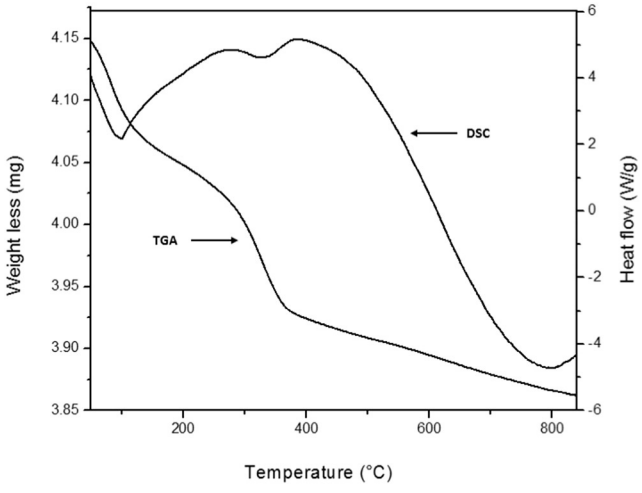


**Fig. 7 – TGA–DSC curves of $CO_2$ adsorption on MgO-BM2.5h sample. DSC: differential scanning calorimetry.**

Please cite this article as: Elvira, G.-B., et al., MgO-based adsorbents for $CO_2$ adsorption: Influence of structural and textural properties on the $CO_2$ adsorption performance, J. Environ. Sci. (2016), http://dx.doi.org/10.1016/j.jes.2016.11.016

surface adsorbed) at 3433 $cm^{-1}$ are generally attributed to strong hydrogen bound OH species that are usually found in MgO even after vacuum drying (Yan et al., 2009). The band at 2314 $cm^{-1}$ after $CO_2$ adsorption (Fig. 8c) indicates the existence of physisorbed carbon dioxide (Ding et al., 2015). Small band at 2314 $cm^{-1}$ also was found in Fig. 8a and b, it should be expected that this 2314 $cm^{-1}$ band disappears in degassed MgO-BM2.5h sample (Fig. 8b), however, the 2314 $cm^{-1}$ band for fresh material was very much smaller due to their large manipulation time for IR measurement or by hygroscopic nature of MgO. By examination of 1200 to 1700 $cm^{-1}$ region, three different unidentate, bidentate and bicarbonate species of adsorbed $CO_2$ were detected. According to Pighini et al. (2011), unidentate and bidentate carbonate formation requires surface basic oxygen atoms, in our study, unidentate carbonates were exhibited at 1280 and 1490 $cm^{-1}$ adsorption bands. Bidentate carbonate stretching at 878 and 1560 $cm^{-1}$ adsorption bands. Finally, bicarbonate species that involves surface hydroxyl groups were exhibited at 1630 and 1417 $cm^{-1}$ adsorption bands. IR revealed the formation of $MgCO_3$ in the adsorbent studied here. Then, based on these results, it is further demonstrated that the adsorption mechanism of the MgO-BM2.5h sample was mainly relying on chemisorption accompanying with a very small fraction of physisorption according to Song et al. (2015).

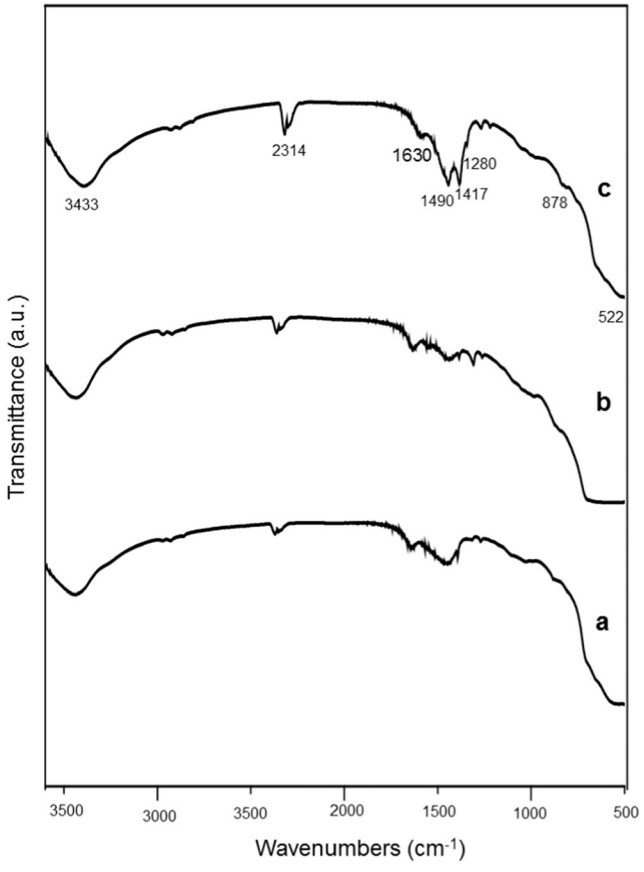


**Fig. 8 – FT-IR spectra of: (a) MgO-BM2.5h without further treatment, (b) MgO-BM2.5h with degassed treatment at 325°C during 30 min, and (c) $CO_2$ adsorption on MgO-BM2.5h at 25°C and 1 atm. FT: fourier transform; IR: infrared.**

To evaluate the reuse and stability of MgO-BM2.5h-based adsorbent for practical applications, experiments of adsorption–desorption cycles on this sample were repeated five times. $CO_2$ adsorption was carried out at 25°C, 1 atm, and 30 min of saturation time. $CO_2$ desorption was carried out by using TGA from 0 to 850°C, with a heating ramp of 20°C/min. According to Wang et al. (2014), this study is necessary because long-time stability of an adsorbent is a critical parameter for the commercialization of a $CO_2$ scavenger. It is well-known that the characteristic of an adsorbent in a practical application point of view is its useful life-time, because longer period of time brings to a meaningful decrease in cost of the synthesis. Fig. 9 shows the cyclical capacity of MgO-BM2.5h powders, this sample exhibited a $CO_2$ adsorption capacity of 1.47 mmol/g at 5th cycle, equivalent to 91.3% of the obtained capacity in 1st cycle (1.61 mmol/g). Then, the cyclic $CO_2$ adsorption–desorption showed that MgO-BM2.5h sample maintains high stability in cyclic capacity, beneficial properties for its economical and practical applications as $CO_2$ adsorbent.

The methods reported here are advantageous because the solution–combustion synthesis is a versatile process that with only 5 min allows to synthesize MgO powders of improved textural properties, which play an important role for $CO_2$ adsorption efficiency. Besides, the ball-milling allowed one resulting product of very fine particulates, with strain and defects forming friable agglomerates improving their textural and structural properties that enhanced $CO_2$ adsorption efficiency on MgO powders. In summary, in this work the $CO_2$ adsorption on MgO obtained by solution combustion and treated by ball-milling at room temperature and pressure conditions has been demonstrated, which has not been reported previously. Therefore, a better understanding of textural and structural influence properties of the as-prepared porous MgO-based adsorbents on the $CO_2$ adsorption behavior was attained, as a contribution of alleviating the serious global warming problem.

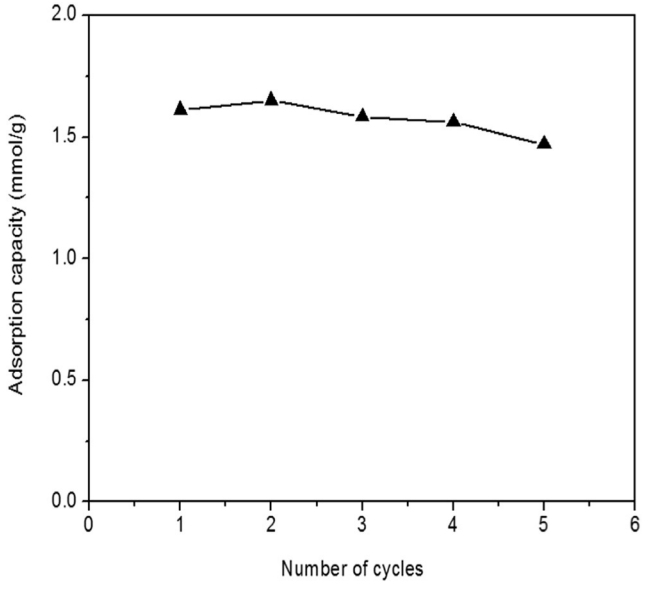


**Fig. 9 – Cyclic test of $CO_2$ adsorption on MgO-BM2.5h sample at 25°C and 1 atm.**

Please cite this article as: Elvira, G.-B., et al., MgO-based adsorbents for $CO_2$ adsorption: Influence of structural and textural properties on the $CO_2$ adsorption performance, J. Environ. Sci. (2016), http://dx.doi.org/10.1016/j.jes.2016.11.016

## 3. Conclusions

In the present investigation, mesoporous MgO-based adsorbents were synthesized successfully by solution–combustion and ball-milling processes, likewise were mixed with Fe and Ni elements to obtain their respective nanocomposites, and their $CO_2$ adsorption behaviors were investigated. Experimental results revealed that MgO-based adsorbent obtained by solution–combustion was crystalline, highly porous with extended specific surface area. However, when this resulted MgO material was ball-milling treated during 2.5 hr (MgO-BM2.5h), their textural and structural properties were improved. The results show that this MgO-BM2.5h adsorbent was able to adsorb $CO_2$ very well at room temperature and pressure with a maximum $CO_2$ adsorption capacity of 1.611 mmol/g. After the introduction of Fe and Ni into MgO, Fe had a negligible influence on $CO_2$ adsorption behavior, in comparison with the favorable influence of Ni into MgO sample. Chemisorption was the main mechanism for $CO_2$ adsorption on mesoporous MgO-BM2.5h, accompanying with a very small fraction of physisorption which was probed by FTIR study. $CO_2$ adsorption behavior on MgO-based adsorbents was correlated with their structural, textural and structural properties as: specific surface area, total pore volume, pore size distribution and crystallinity. The recyclability of the mesoporous MgO-BM2.5h adsorbent is highly commendable, because no significant loss of performance was measured until five regeneration times. In general, the results indicate that the ball-milling process plays a crucial role in the obtaining of highly porous MgO with better textural and structural properties for enhancing the $CO_2$ adsorption capacity.

## Acknowledgments

The authors are grateful to the National Institute of Nuclear Research (ININ), México, for financial support through project CB-406 stages I–III. Elvira Gutiérrez Bonilla is grateful to National Council for Science and Technology (CONACyT), México, for the scholarship granted.

## REFERENCES

Abanades, J.C., Anthony, E.J., Wang, J., Oakey, J.E., 2005. Fluidized bed combustion systems integrating $CO_2$ capture with CaO. Environ. Sci. Technol. 39 (8), 2861–2866.

Abd-El-Hafiz, D.R., Riad, M., Mikhail, S., 2015. Nano-structured Mn–Al and Co–Al oxide materials for catalytic ethanol conversion. J. Nanostruct. Chem. 5 (4), 393–403.

Adelkhani, H., Ghaemi, M., Ruzbehani, M., 2011. Evaluation of the porosity and the nano-structure morphology of $MnO_2$ prepared by pulse current electrodeposition. Int. J. Electrochem. Sci. 6, 123–135.

Bai, J., Meng, F., Wei, C., Zhao, Y., Tan, H., Liu, J., 2011. Solution combustion synthesis and characteristics of nanoscale MgO powders. Ceramics-Silikáty 55 (1), 20–25.

Bhagiyalakshmi, M., Lee, J.Y., Jang, H.T., 2010. Synthesis of mesoporous magnesium oxide: its application to $CO_2$ chemisorption. Int. J. Greenh. Gas Con. 4 (1), 51–56.

Bhagiyalakshmi, M., Hemalatha, P., Ganesh, M., Mei, P., Jang, H.T., 2011. A direct synthesis of mesoporous carbon supported MgO sorbent for $CO_2$ capture. Fuel 90 (4), 1662–1667.

Bhatta, L.K.G., Subramanyam, S., Chengala, M.D., Olivera, S., Venkatesh, K., 2015. Progress in hydrotalcite like compounds and metal-based oxides for $CO_2$ capture: a review. J. Clean. Prod. 103, 171–196.

Busca, G., Lorenzelli, V., 1982. Infrared spectroscopic identification of species arising from reactive adsorption of carbon oxides on metal oxide surfaces. J. Mater. Chem. 7 (1), 89–126.

Cai, W.Q., Yu, J.G., Mann, S., 2009a. Template-free hydrothermal fabrication of hierarchically organized γ-AlOOH hollow microspheres. Microporous Mesoporous Mater. 122 (1–3), 42–47.

Cai, W.Q., Yu, J.G., Cheng, B., Su, B.L., Jaroniec, M., 2009b. Synthesis of boehmite hollow core/shell and hollow microspheres via sodium tartrate-mediated phase transformation and their enhanced adsorption performance in water treatment. J. Phys. Chem. C 113 (33), 14739–14746.

Choong-Hwan, J., Ji-Yeon, P., 2010. Highly sinterable nanocrystalline yttria powders fabricated by solution combustion synthesis. J. Ceram. Process. Res. 11 (6), 698–700.

Crittenden, J.C., Trussel, R.R., Hand, D.W., Howe, K.J., Tchobanoglous, G., 2005. Water Treatment: Principles and Design. second ed. John Wiley and Sons, New Jersey.

Devaraja, P.B., Avadhani, D.N., Prashantha, S.C., Nagabhushana, H., Sharma, S.C., Nagabhushana, B.M., et al., 2014. Synthesis, structural and luminescence studies of magnesium oxide. Spectrochim. Acta A Mol. Biomol. Spectrosc. 118, 847–851.

Ding, Y., Song, G., Zhu, X., Chen, R., Liao, Q., 2015. Synthesizing MgO with a high specific surface for carbon dioxide adsorption. RSC Adv. 5, 30929–30935.

Ello, A., de Souza, L., Trokourey, A., Jaroniec, M., 2013. Development of microporous carbons for $CO_2$ capture by KOH activation of African palm shells. J. $CO_2$ Util. 2, 35–38.

Granados-Correa, F., Bonifacio-Martínez, J., 2014. Combustion synthesis process for the rapid preparation of high-purity SrO powders. Mater. Sci. Pol. 32 (4), 682–687.

Granados-Correa, F., Bonifacio-Martínez, J., Lara, V.H., Bosch, P., Bulbulian, S., 2008. Cobalt sorption properties of MgO prepared by solution combustion. Appl. Surf. Sci. 254 (15), 4688–4694.

Granados-Correa, F., Bonifacio-Martínez, J., Hernández-Mendoza, H., Bulbulian, S., 2016. Capture of $CO_2$ on γ-$Al_2O_3$ materials prepared by solution–combustion and ball-milling processes. J. Air Waste Manage. Assoc. 66 (7), 643–654.

Harrison, D.P., 2004. The role of solids in $CO_2$ capture: a mini review. Proceedings of the 7th International Conference on Greenhouse Gas Control Technologies Vancouver, Canada., pp. 1101–1106

Houshmand, A., Daud, W., Lee, M., Shafeeyan, M., 2012. Carbon dioxide capture with amine-grafted activated carbon. Water Air Soil Pollut. 223 (2), 827–835.

Jain, S.R., Adiga, K.C., 1981. A new approach to thermochemical calculations of condensed fuel-oxidizer mixtures. Combust. Flame 40, 71–79.

Janet, C.M., Viswanathan, B., Viswanath, R.P., Varadarajan, T.K., 2007. Characterization and photoluminescence properties of MgO microtubes synthesized from hydromagnesite flowers. J. Phys. Chem. C 111 (28), 10267–10272.

Janusz, W., Khalameida, S., Sydorchuk, V., Skwarek, E., Zazhigalov, V., Skubiszewska, Z.J., et al., 2010. Some properties of milled vanadium phosphates. Adsorption 16 (4), 333–341.

Jeong, M., Kim, S.Y., Kim, D.H., Han, S.W., Kim, I.H., Lee, M., Hwang, Y.K., Kim, Y.D., 2016. High-performing and durable MgO/Ni catalysts via atomic layer deposition for $CO_2$ reforming of methane (CRM). Appl. Catal. A. Gen. 515, 45–50.

Jin, C., Kim, H., Park, S., Lee, C., 2012. Synthesis of biaxial MgO/Mg–Sn–O nanowire heterostructures and their structural and luminescence properties. J. Alloys Compd. 541, 163–167.

Please cite this article as: Elvira, G.-B., et al., MgO-based adsorbents for $CO_2$ adsorption: Influence of structural and textural properties on the $CO_2$ adsorption performance, J. Environ. Sci. (2016), http://dx.doi.org/10.1016/j.jes.2016.11.016

Khajenoori, M., Rezaei, M., Meshkani, F., 2015. Dry reforming over $CeO_2$-promoted Ni/MgO nanocatalyst: effect of Ni loading and $CH_4/CO_2$ molar ratio. J. Ind. Eng. Chem. 21, 717–722.

Kim, J.Y., Jung, H.S., Hong, K.S., 2005. Effects of acetic acid on the crystallization temperature of sol–gel derived MgO nano-powders and thin films. J. Am. Ceram. Soc. 88 (3), 784–787.

Kumar, S., Saxena, S.K., 2014. A comparative study of $CO_2$ sorption properties for different oxides. Mater. Renew. Sustain. Energy 30 (3), 1–15.

Kumar, S., Saxena, S.K., Drozd, V., Durygin, A., 2015. An experimental investigation of mesoporous MgO as a potential pre-combustion $CO_2$ sorbent. Mater. Renew. Sustain. Energy 4 (8), 1–8.

Li, L., Wen, X., Fu, X., Wang, F., Zhao, N., Xiao, F.K., et al., 2010. $MgO/Al_2O_3$ sorbent for $CO_2$ capture. Energy Fuel 24 (10), 5773–5780.

Liang, G., Hout, J., Schultz, R., 2001. Hydrogen storage properties of mechanically alloyed LaNi5-based materials. J. Alloys Compd. 320 (1), 133.

Liu, J., Thallapally, P.K., McGrail, B.P., Brown, D.R., 2012. Progress in adsorption-based $CO_2$ capture by metal–organic frameworks. Chem. Soc. Rev. 41 (6), 2308–2322.

Maliyekkal, S.M., Anshup, A.K.R., Pradeep, T., 2010. High yield combustion synthesis of nanomagnesia and its application for fluoride removal. Sci. Total Environ. 408, 2273–2282.

Mantilaka, M.M.M.G.P.G., Pitawala, H.M.T.G.A., Karunaratne, D.G.G.P., Rajapakse, R.M.G., 2014. Nanocrystalline magnesium oxide from dolomite via poly(acrylate) stabilized magnesium hydroxide colloids. Colloids Surf. A. Physicochem. Eng. Asp. 443, 201–208.

Pighini, C., Belin, T., Mijoin, J., Magnoux, P., Costentin, G., Lauron-Pernot, H., 2011. Microcalorimetric and thermodynamic studies of $CO_2$ and methanol adsorption on magnesium oxide. Appl. Surf. Sci. 257, 6952–6962.

Radosław, D., Radlikc, M., Motaka, M., Galvez, M.E., Turekc, W., Costab, P., et al., 2015. Ni-containing Ce-promoted hydrotalcite derived materials as catalysts for methane reforming with carbon dioxide at low temperature-on the effect of basicity. Catal. Today 257 (1), 59–65.

Rao, K.V., Sunandana, C.S., 2008. Structure and microstructure of combustion synthesized MgO nanoparticles and nanocrystalline MgO thin films synthesized by solution growth route. J. Mater. Sci. 43 (1), 146–154.

Ross, J.R.H., 2005. Natural gas reforming and $CO_2$ mitigation. Catal. Today 100, 151–158.

Saiwana, C., Muchana, P., Montigny, D., Tontiwachwutikul, P., 2014. New poly (vinylbenzylchloride/divinylbenzene) adsorbent for carbon dioxide desorption. II. Effect of amine. Energy Procedia 63, 2317–2322.

Shafeeyan, M., Wan, D., Shamiri, A., Aghamohammadi, N., 2015. Adsorption equilibrium of carbon dioxide on ammonia-modified activated carbon. Chem. Eng. Res. Des. 104, 42–52.

Singh, S., Barick, K.C., Bahadur, D., 2013. Functional oxide nanomaterials and nanocomposites for the removal of heavy metals and dyes. Nanomater. Nanotechnol. 3, 1–19.

Singh, V., Sharma, A.K., Sanghi, R., 2009. Poly(acrylamide) functionalized chistosan: an efficient adsorbent for azo dyes from aqueous solutions. J. Hazard. Mater. 166 (1), 327–335.

Siriwardane, R., Shen, M., Fisher, E., 2005. Adsorption of $CO_2$ on zeolites at moderate temperatures. Energy Fuel 19 (3), 1153–1159.

Song, G., Ding, Y., Zhu, X., Liao, Q., 2015. Carbon dioxide adsorption characteristics of synthesized MgO with various porous structure achieved by varying calcination. Colloids Surf. A: Physicochem. Eng. Aspect 470, 39–45.

Song, G., Zhu, X., Chen, R., Liao, Q., Ding, Y., Chen, L., 2016. An investigation of $CO_2$ adsorption kinetics on porous magnesium oxide. Chem. Eng. J. 283, 175–183.

Toniolo, J.C., Takimi, A.S., Bergmann, C.P., 2010. Nanostructured cobalt oxides ($Co_3O_4$ and CoO) and metallic Co powders synthesized by the solution combustion method. Mater. Res. Bull. 45 (6), 672–676.

Valverde, J.M., Sanchez-Jimenez, P.E., Perez-Maqueda, L.A., Quintanilla, M.A.S., Perez-Vaquero, J., 2014. Role of crystal structure on $CO_2$ capture by limestone derived CaO subjected to carbonation/recarbonation/calcination cycles at Ca-looping. Appl. Energy 125, 264–275.

Vu, A.T., Park, Y., Jeon, P.R., Lee, C.H., 2014. Mesoporous MgO sorbent promoted with $KNO_3$ for $CO_2$ capture at intermediate temperatures. Chem. Eng. J. 258, 254–264.

Wang, Q.A., Luo, J.Z., Zhong, Z.Y., Borgna, A., 2011. $CO_2$ capture by solid adsorbents and their applications: current status and new trends. Energy Environ. Sci. 4, 42–55.

Wang, B., Yan, R., Liu, H., 2012. Effects of interactions between NiM (M = Mn, Fe, Co and Cu) bimetals with MgO (100) on the adsorption of $CO_2$. Appl. Surf. Sci. 258 (22), 8831–8836.

Wang, K., Wang, X., Zhao, P., Guo, X., 2014. High-temperature capture of $CO_2$ on lithium-based sorbents prepared by a water-based sol–gel technique. Chem. Eng. Technol. 37 (9), 1552–1558.

Yan, H., Zhang, X., Wei, L., Liu, X., Xu, B., 2009. Hydrophobic magnesium hydroxide nanoparticles via oleic acid and poly(methyl methacrylate)-grafting surface modification. Powder Technol. 193 (2), 125–129.

Zhao, Z., Dai, H., Du, Y., Deng, J., Zhang, L., Shi, F., 2011. Solvo- or hydrothermal fabrication and excellent carbon dioxide adsorption behaviors of magnesium oxides with multiple morphologies and porous structures. Mater. Chem. Phys. 128 (3), 348–356.

Please cite this article as: Elvira, G.-B., et al., MgO-based adsorbents for $CO_2$ adsorption: Influence of structural and textural properties on the $CO_2$ adsorption performance, J. Environ. Sci. (2016), http://dx.doi.org/10.1016/j.jes.2016.11.016